AD-A137 829 GLOBAL PNS (PARABOLIZED NAVIER-STOKES) SOLUTIONS FOR LAMINAR AND TURBULEN..(U) CINCINNATI UNI OH DEPT OF AEROSPACE ENGINEERING AND APPLIED M.. S G RUBIN ET AL. 1/1

UNCLASSIFIED JUL 83 AFOSR-TR-84-0028 AFOSR-80-0047 F/G 20/4 NL

END

FILMED

3-84

DTIC

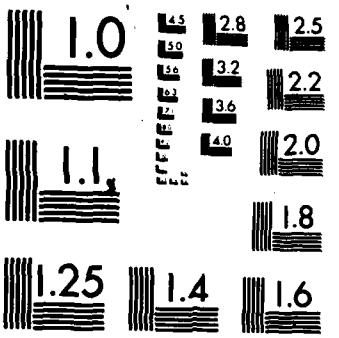

MICROCOPY RESOLUTION TEST CHART
NATIONAL BUREAU OF STANDARDS-1963-A

UNCLASSIFIED

SECURITY CLASSIFICATION OF THIS PAGE (When Data Entered)

REPORT DOCUMENTATION PAGE		READ INSTRUCTIONS BEFORE COMPLETING FORM
1. REPORT NUMBER AFOSR-TR- 84-0028	2. GOVT ACCESSION NO. AD-A137829	3. RECIPIENT'S CATALOG NUMBER
4. TITLE (and Subtitle) GLOBAL PNS SOLUTIONS FOR LAMINAR AND TURBULENT FLOW		5. TYPE OF REPORT & PERIOD COVERED INTERIM 6. PERFORMING ORG. REPORT NUMBER
7. AUTHOR(s) S G RUBIN D R REDDY		8. CONTRACT OR GRANT NUMBER(s) AFOSR-80-0047
9. PERFORMING ORGANIZATION NAME AND ADDRESS UNIVERSITY OF CINCINNATI DEPT OF AEROSPACE ENGINEERING & APPLIED MECHANICS CINCINNATI, OH 45221		10. PROGRAM ELEMENT, PROJECT, TASK AREA & WORK UNIT NUMBERS 61102F 2307/A1
11. CONTROLLING OFFICE NAME AND ADDRESS AIR FORCE OFFICE OF SCIENTIFIC RESEARCH/NA BOLLING AFB, DC 20332		12. REPORT DATE July 1983 13. NUMBER OF PAGES 11
14. MONITORING AGENCY NAME & ADDRESS(if different from Controlling Office)		15. SECURITY CLASS. (of this report) Unclassified 15a. DECLASSIFICATION/DOWNGRADING SCHEDULE

16. DISTRIBUTION STATEMENT (of this Report)

Approved for Public Release; Distribution Unlimited.

17. DISTRIBUTION STATEMENT (of the abstract entered in Block 20, if different from Report)

18. SUPPLEMENTARY NOTES

Proceedings of the AIAA Computational Fluid Dynamics Conference, 6th Danvers, Massachusetts 13-15 July 1983, The American Institute of Aeronautics & Astronautics, 1983

19. KEY WORDS (Continue on reverse side if necessary and identify by block number)

PARABOLIZED NAVIER-STOKES EQUATIONS
RELAXATION PROCEDURE
LAMINAR FLOW
TURBULENT FLOW
SEPARATED FLOW

20. ABSTRACT (Continue on reverse side if necessary and identify by block number)

A multi-sweep relaxation procedure is applied for inviscid and parabolized (pressure-elliptic) Navier-Stokes (PNS) equations. Boattail, finite flat plate and NASA 0012 airfoil geometries are considered for incompressible and subsonic inviscid, laminar and turbulent flow. The equations are written in a conformal body-fitted coordinate frame and differenced on a staggered grid in order to give second-order accuracy for the inviscid flow and somewhere between first and second-order accuracy for the PNS solutions. A full second-order scheme is also discussed. Separation, trailing edge

DD FORM 1 JAN 73 1473 EDITION OF 1 NOV 65 IS OBSOLETE

UNCLASSIFIED

SECURITY CLASSIFICATION OF THIS PAGE (When Data Entered)

and stagnation point flow are evaluated. The effects of normal pressure gradients for laminar and turbulent flows are compared. A multi-grid procedure is applied in order to speed convergence rates for fine meshes and/or large computational domains.

Reprinted from CP834, a Bound Collection of Technical Papers

AIAA-83-1911
Globl PNS Solutions for Laminar and Turbulent Flow

S.G. RUBIN and D.R. REDDY

AIAA 6th COMPUTATIONAL FLUID DYNAMICS CONFERENCE

July 13-15, 1983 / Danvers, Massachusetts

GLOBAL PNS SOLUTIONS FOR LAMINAR AND TURBULENT FLOW

S.C. Rubin* and D.R. Reddy**

University of Cincinnati
Cincinnati, Ohio 45221

Abstract

A multi-sweep relaxation procedure is applied for inviscid and parabolized (pressure-elliptic) Navier-Stokes (PNS) equations. Boattail, finite flat plate and NACA 0012 airfoil geometries are considered for incompressible and subsonic inviscid, laminar and turbulent flow. The equations are written in a conformal body fitted coordinate frame and differenced on a staggered grid in order to give second-order accuracy for the inviscid flow and somewhere between first and second-order accuracy for the PNS solutions. A full second-order scheme is also discussed. Separation, trailing edge and stagnation point flow are evaluated. The effects of normal pressure gradients for laminar and turbulent flows are compared. A multi-grid procedure is applied in order to speed convergence rates for fine meshes and/or large computational domains.

1. Introduction

The reduced form of the Navier-Stokes equations originally termed parabolized Navier-Stokes (PNS) and more recently semi-elliptic, partially parabolic or thin layer are considered herein by relaxation methods for the evaluation of incompressible and subsonic flows with strong pressure interaction and/or separation. Previous analysis by the authors and solutions for laminar incompressible flow for trough and boattail configurations are given in references 1-4, for subsonic and transonic flow over a cone-cylinder-boattail geometry in references 6, 7 and for supersonic flow over a cone in reference 8. The present procedure is applicable to inviscid as well as viscous interacting flow and can be classified as intermediary between interacting boundary layer theory and conventional Navier-Stokes or PNS technique.

The PNS equations were first applied for hypersonic problems[9,10] where the contribution of the pressure gradient p_x in the longitudinal (x) momentum equation is negligible and can be neglected. The system is then mathematically parabolic and can be solved as an initial value problem by marching techniques. For lower Mach numbers, where p_x must be retained, an elliptic influence associated with the pressure interaction through the subsonic portion of boundary layer appears in the PNS system.[10,11] Single sweep marching then leads to an ill-posed initial value problem[10-12] and exponentially growing departure solutions appear for step sizes $\Delta x > (\Delta x)_{min}$, where $(\Delta x)_{min}$ is proportional to the extent of the subsonic portion of the flow.[8,12]

Alternatively, an eigenvalue analysis[13] has shown that the p_x term can be structured so that $p_x = \omega(p_x)_p + (1-\omega)(p_x)_e$, where $\omega(M)$ is a function of a local Mach number M and $0 \le \omega \le 1$, $\omega(0) = 0$, $\omega(1) = 1$. The term $\omega(p_x)_p$ represents the parabolic (marching) contribution to p_x and $(1-\omega)(p_x)_e$ represents the elliptic contribution to p_x. This latter term contains the upstream influence. If included in a marching calculation where the $M > 1$, the ill-posedness of the initial value problem is once again in apparent with the appearance of the departure solutions that reflect different downstream boundary conditions for the pressure. The $(\Delta x)_{min}$ and $\omega(p_x)_p$ descriptions can be reconciled by defining Δx as $\Delta\bar{x}/\omega$ in the general marching analysis. For given $\Delta\bar{x}$, $\omega(M)$ and therefore Δx vary across the subsonic layer in order to obtain departure free marching solutions. This procedure is inconsistent for flows where p_x is important.

In recent papers by the authors,[1-5] it has been shown that for incompressible flow, $(\Delta x)_{min}$ is proportional to the total extent of the computational boundary y_M in the surface normal direction. This implies that for $y_M \to \infty$, $(\Delta x)_{min} \to \infty$, or with $\omega(0) = 0$ the entire p_x contribution is elliptic and therefore must be neglected for departure free single sweep marching procedures. For subsonic flows, $\omega \ll 1$ over a range of y values so that $(\Delta x)_{min} \gg 1$. However, from the p_x split of reference 13, shown previously, it is seen that $(\Delta x)_{min}$ for subsonic flow is reduced by the factor $(1-\omega)$ over the value obtained in references 2-5 for incompressible flow, i.e., $(\Delta x)_{min} \sim (1-\omega)(\Delta x)_{min/M=0}$.

In order to circumvent the ill-posedness of single sweep PNS methods, a global pressure relaxation or multiple marching procedure has been proposed by the authors[1-8] for the entire Mach number range, i.e., incompressible to supersonic flow. This requires an appropriate and exact "forward" or mid-point difference treatment of the p_x contribution since this term alone (for attached flow) contains the upstream or elliptic influence. Significantly, only the pressure (and velocities in in regions of reversed flow) must be stored during the relaxation process. This leads to a significant reduction over conventional Navier-Stokes and PNS methods.

Consistent (Δx arbitrary), departure free ($\Delta x > 0$) and rapidly convergent solutions have previously been obtained for laminar incompressible,[1-5] subsonic,[6] transonic[7] and weakly interacting supersonic[8] flows. Strong pressure interactions and separation have been captured with the global PNS procedure. Several differencing procedures, the stability of single pass and global relaxation and an analysis of the effective poisson pressure and vorticity equations has been presented in earlier studies.[3-5]

---

* Head and Professor, Dept. of Aerospace Engineering and Applied Mechanics, Member AIAA.

**Research Associate, Dept. of Aerospace Engineering and Applied Mechanics.

In the present paper, the difference equations describing the PNS equations are defined on a partially staggered grid. This leads to a modified interpretation of the discrete p_x approximation. A multi-grid line relaxation procedure that reduces computer effort and storage is outlined. The convergence properties and the accuracy of the discrete system is discussed for inviscid, laminar and turbulent modelling. The applicability of the relaxation procedure is demonstrated for inviscid flow. Convergence studies are presented for an axisymmetric boattail configuration. Incompressible and low speed compressible flow results are then discussed for laminar and turbulent flow over a finite flat plate and a NACA 0012 airfoil at zero incidence. Of particular interest is the behavior near the trailing edge, the stagnation point and in regions of separation. In addition, the importance of the normal pressure gradients in these regions will be compared for laminar and turbulent flow conditions.

2. Governing Equations

The governing PNS system considered here is written in a conformal coordinate frame (ξ,η) for the primitive variables, pressure p, density ρ, temperature T, viscosity coefficient μ, and velocities u,v. The transformed cartesian coordinates $\xi = \xi(x,y)$ along the surface and $\eta = \eta(x,y)$ normal to the surface are related to the (x,y) physical coordinates through the transformation $z = f(z)$, where $z = \xi+i\eta$ and $z = x+iy$. The metric $h = |f'(z)|$ and $h_\xi - ih_\eta = h(f''/f)$. The metric $h_3 = y^\epsilon$, where $\epsilon = 1$ for axisymmetry.

Continuity

$$(\rho hy^\epsilon u)_\xi + (\rho hy^\epsilon v)_\eta = 0 \qquad (1)$$

ξ-momentum

$$\frac{1}{hy^\epsilon}(\rho hy^\epsilon u^2)_\xi + \frac{1}{hy^\epsilon}(\rho uvhy^\epsilon)_\eta + (\rho uvh)_\eta/h - (\rho uv)_\eta - (\rho v^2 h)_\xi/h + (\rho v^2)_\xi = -p_\xi + \frac{1}{v^\epsilon}\left[\frac{v^\epsilon}{h^2}\mu(hu)_\eta\right]_\eta \qquad (2)$$

η-momentum

$$-p_\eta = (\rho uvhy^\epsilon)_\xi/hy^\epsilon + (\rho uvh)_\xi/h - (\rho uv)_\xi + \frac{1}{hy^\epsilon}(\rho v^2 hy^\epsilon)_\eta - (\rho u^2 h)_\eta/h + (\rho u^2)_\eta \qquad (3)$$

Energy

$$H = C_p T + \frac{u^2+v^2}{2} = H_\infty = \text{constant} \qquad (4)$$

State;Viscosity

$$p = \rho RT; \quad \mu = \mu(T) \qquad (5)$$

For the present study only adiabatic conditions are considered.

As explained in greater detail in earlier studies[2,3] the version of the PNS equations defined here neglects longitudinal diffusion effects in the ξ-momentum equation (2), as well as all diffusion terms in the normal (η) momentum equation (3); these terms, in the appropriate streamline coordinate frame, are no more important than those already neglected in (2). The continuity (1) and normal momentum equations are then first-order in η (for v and p), so that two-point trapezoidal rule differencing is applied. Conventional three-point differences are considered for ξ-momentum (2). Equations (1-3) are coupled for the variables (u,v,p). The density is obtained through an iterative process at each ξ location, see references 6-8. This allows for a simplification in the treatment of the p_x term and works quite well up to transonic speeds.

3. Difference Equations and Solution Technique

The equations (1-5) are differenced on the staggered grid of figure 1 as shown for incompressible flow.

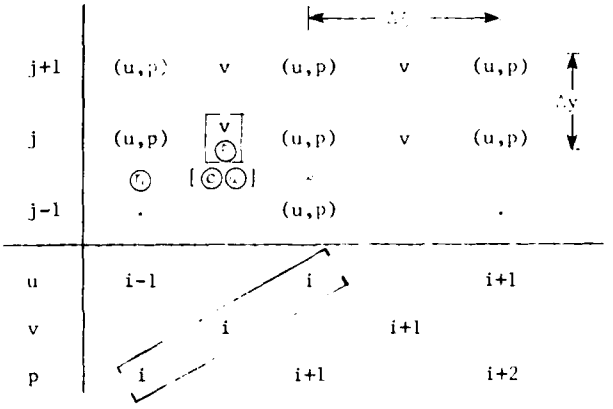

Fig. 1. Staggered Grid - Incompressible Flow.

Both first- and second-order accurate systems of discrete equations have been developed.[3-5] Significantly, the first-order system given below, as equations (6-8), is, in fact, second-order accurate for incompressible inviscid flow. This is particularly important as the PNS system is used to evaluate both viscous and inviscid regions. Therefore, we would expect that overall accuracy will fall somewhere between first and second order. This will be demonstrated in the following sections. The full second-order system is given in references 3-5, and will not be repeated here. This system is more complex, requires many more operations and is very sensitive to coordinate transformation, regions of large curvature, or large longitudinal gradients as in the trailing edge flow. The accuracy of this system has been tested for a semi-infinite flat plate where these effects are negligible. The second-order character of the error has been confirmed.[5] However, for the reasons already cited, the "first"-order or "one and one-half"-order system[6-8] is considered more suitable for the present applications. The equations are shown here for simplicity in non-conservation cartesian coordinates for the flat plate geometry and a uniform mesh in x and y. In fact, non-uniform meshes, conservation equations and conformal

coordinates are used throughout.

Continuity: centered at ⓒ on figure 1

$$[(\rho u)_{i,j} - (\rho u)_{i-1,j} + (\rho u)_{i,j-1} - (\rho u)_{i-1,j-1}]/2 + \frac{\Delta x}{\Delta y}[(\rho v)_{i,j} - (\rho v)_{i,j-1}] = 0 \quad (6)$$

ξ-momentum: centered at ⓢ

$$(\rho u)_{i,j}(u_{i,j}-u_{i-1,j}) + (\rho v)_{i,j}\frac{\Delta x}{2\Delta y}(u_{i,j+1}-u_{i,j-1}) + p^{n-1}_{i+1,j} - p_{i,j} = \frac{\Delta x \mu_{i,j+\frac{1}{2}}}{\Delta y^2}(u_{i,j+1}-u_{i,j}) - \frac{\Delta x \mu_{i,j-\frac{1}{2}}}{\Delta y^2}(u_{i,j}-u_{i,j-1}) \quad (7)$$

η-momentum: centered at ⓝ

$$[\frac{(\rho u)_{i,j}+(\rho u)_{i,j-1}}{4\Delta x}][v_{i,j}-v_{i-1,j}+v_{i,j-1}-v_{i-1,j-1}] + (\frac{(\rho v)_{i,j}+(\rho v)_{i,j-1}}{2\Delta y})(v_{i,j}-v_{i,j-1}) + \frac{p_{i,j}-p_{i,j-1}}{\Delta y} = 0 \quad (8)$$

The equations (6-8) represent a coupled system for the vector $\begin{pmatrix} u \\ v \\ p \end{pmatrix}_{i,j}$. As seen from the unknown bracketed vector in figure 1, on the staggered grid the pressure $p_{i,j}$ is evaluated one grid point upstream of the unknown velocity $u_{i,j}$. This reflects the upstream influence or elliptic effect of the p_ξ term. The superscript n-1 for $p_{i+1,j}$ in (7) denotes the value of the previous global iteration or sweep. The current iteration is designated by n; although, this superscript has been dropped throughout. It is significant that only the pressure term $p^{n-1}_{i+1,j}$ is relaxed during the iteration procedure. Therefore, only $p_{i,j}$ need be stored. For separated flow the convective terms are upwinded so that $u^{n-1}_{i+1,j}$ and $v^{n-1}_{i+1,j}$ are also required, but only in the limited regions of reverse flow.

The treatment of p_ξ in (7) as $(p^{n-1}_{i+1,j}-p^{n}_{i,j})/\Delta\xi$ corresponds to a fully elliptic approximation. From previous studies by the authors, as well as the eigenvalue analysis of reference 13, this description is exact only for incompressible (ω=0) flow. For subsonic flow, the structure discussed in the Introduction, where p_ξ is of the form

$$p_\xi = \omega(p^{n}_{i,j} - p^{n}_{i-1,j})/\Delta\xi + (1-\omega)(p^{n-1}_{i+1,j}-p^{n}_{i,j})/\Delta\xi \quad (9)$$

should apply if the density is coupled with the (u,v,p) calculation. However, if the density is treated iteratively, as in the artificial compressibility procedure for transonic flow, it is possible to consider the fully elliptic (ω=0) form for p_ξ. This has been applied for subsonic,[6] transonic[7] and supersonic[8] cases. For supersonic flows with $\Delta\xi/y_M \ll 1$, convergence will however be slower than with the exact treatment of (9). In this procedure $p_{i,j}$ and $p_{i+1,j}$ are always located at the positions shown on figure 1. For supersonic regions the exact differencing would be $p_\xi = (p^{n}_{i+1,j}-p^{n}_{i,j})/\Delta\xi$, so that the error is of the form $(p^{n}_{i+1,j}-p^{n-1}_{i+1,j})/\Delta\xi$, i.e. an iterative time term that vanishes when convergence is achieved.

If the exact treatment (9) is used with density iteration, then it is appropriate to rewrite (9)

$$p_\xi = \frac{p^{n-1}_{i+1,j} - p^{n}_{i,j}}{\Delta\xi} - \omega(\frac{p^{n-1}_{i+1,j} - 2p^{*n}_{i,j} + p^{n}_{i-1,j}}{\Delta\xi}) \quad (10)$$

where the (*) denotes the latest local iterative value during the n^{th} global iteration. For ω=1, at local convergence

$$p_\xi = \frac{p^{n}_{i,j} - p^{n}_{i-1,j}}{\Delta\xi} \quad .$$

In this procedure, the pressure at the $u_{i,j}$ location of figure 1 becomes $\omega p_{i,j}+(1-\omega)p_{i+1,j}$ and global convergence is accelerated for supersonic points. Both methods have been applied successfully here and in references 6-8. Equation (10) is directly obtainable from (9), if $p^{n}_{i+1,j}$ is approximated by $2p^{n}_{i,j} - p^{n}_{i-1,j}$ so that the two approaches differ only in truncation error.

The density, temperature and viscosity coefficient are obtained from (4) and (5). A linear $\mu(T)$ relationship has been assumed herein. When these quantities have been updated the vector $\begin{pmatrix} u \\ v \\ p \end{pmatrix}_{i,j}$ is re-evaluated until some specific degree of convergence, usually 10^{-4} in sequential steps, is achieved. The nonlinear system is quasi-linearized in a standard manner[3-5] and nonlinear terms are updated at the same time as the density, viscosity, etc. After final convergence at location i, the procedure continues to i+1, etc.

The tridiagonal linearized system (6-8) is solved for $\begin{pmatrix} u \\ v \\ p \end{pmatrix}_{i,j}$ by the standard LU decomposition. The total line relaxation procedure continues to the right hand boundary. The (n-1) terms are then updated and the marching process is repeated. The solution procedure is terminated when the changes in maximum pressure and skin friction between global iterations is less than 10^{-4}. Line relaxation is considered most efficient for the present analysis as it minimizes storage requirements. More efficient procedures, such as ADI or CSIP would require increased storage for the velocities as well as the pressure. Since our goal is to reduce storage requirements for future three-

dimensional applications, simple line relaxation with a multi-grid corrector, to be discussed shortly, was chosen.

4. Boundary Conditions

For the primitive variable system (6-8) on the staggered grid of figure 1, the following boundary conditions apply:

At the inflow $\xi = \xi_0$: $u(\xi_0,\eta) = U(\eta)$ and $v(\xi_0,\eta) = V(\eta)$. $V(\eta) = \omega(\eta) + U'(\eta)$, where $\omega(\eta)$ is the inflow vorticity; for uniform conditions $U = 1$ and $V = 0$ (zero vorticity). A condition for the pressure is not required for incompressible flow. As seen from figure 1, the inflow pressure is calculated during the first marching step.

At the upper surface $\eta = \eta_M$: $u = 1$, $p = 1$; i.e., free-stream conditions are applied. This requires that η_M be sufficiently large, e.g., outside of the domain of the triple deck interaction.[3-5] The outer boundary could be moved closer to the surface by applying conditions similar to those of interacting boundary layer theory; however, for the present calculations, the fully inviscid evaluation was included. A boundary condition on v is not required.

At the outflow $\xi = \xi_1$: Only the pressure $p(\xi_1,\eta)$ or derivative $p_\xi(\xi_1,\eta)$ are prescribed. For the present calculations, both $p = 0$ and $p_\xi = 0$ were applicable. There are only slight differences in the solutions.

At the wall $\eta = 0$: For viscous flow $u(\xi,0) = v(\xi,0) = 0$ is specified. For inviscid flow only $v(\xi,0) = 0$ is required. A boundary condition on the pressure is not required.

Significantly pressure boundary conditions are only specified at the upper and outflow boundaries. As shown in references 4,5, the equations (6-8) can be manipulated to provide an effective poisson pressure solver; the remaining pressure boundary conditions, of Neumann type, are implicitly imposed and can be inferred directly from the original difference equations. There is no need to apply the differential form of the poisson equation and derivative boundary conditions only indirectly, as is commonly done for most incompressible flow proce-

[illegible] and Multi-Grid Procedure

[illegible] stability analysis of references [illegible] for incompressible flow [illegible] of the linear matrix [illegible] relaxation procedure is of

[illegible] $_M$ 1 the rate of [illegible] to raise markedly. It is interest- [illegible] parameter [illegible] $_M$ 1, which leads to [illegible] for single sweep methods,[2]

is a convergence factor for the global relaxation procedure. As noted in the previous discussion, from the eigenvalue analysis[13] for subsonic flow, it can be inferred that the convergence condition will be of the form $\lambda \sim (1-\alpha)[1 - A(\frac{\alpha}{M})^2]$. This implies more rapid convergence with large regions of high subsonic or supersonic Mach numbers and fixed α_M, since $\lambda \to 1$ as $M \to 1$.

In order to improve the convergence rate, a one-dimensional (in η) multi-grid procedure following the full approximation scheme of reference (14) has been applied. This approach is less efficient, in terms of storage requirements, than a full two-dimensional multi-grid application; however, relaxation for p is only in the η-direction and the calculation is fully implicit in ξ. Also, a highly non-uniform mesh is required to accurately describe the boundary layer, triple deck and inviscid regions. This is not ideally suited for interpolation required by the multi-grid procedure. Of particular note, error transfer from coarse to fine grids is applied only for the pressure, even in regions of reversed flow where the velocities $u^{n-1}_{i+1,j}$ and $v^{n-1}_{i+1,j}$ are also relaxed. These values are fixed on each grid from the previous global (n-1) iteration. Since the separation zones are of considerably different extent on each grid, the transfer process for the velocities was considered to be a source of possible difficulty. The present procedure works quite well for most of the problems considered here and is discussed in greater detail in references 4,5.

The effects of the multi-grid procedure on the convergence properties are shown in figure 2 for a trough geometry discussed previously in references 4,5. Similar results were found for the flat plate configuration. When large regions of separated flow occur, the coarse grid corrections are less effective and the multi-grid procedure appears to enter a limit cycle. For this reason, the coarse grid solutions were simply applied as

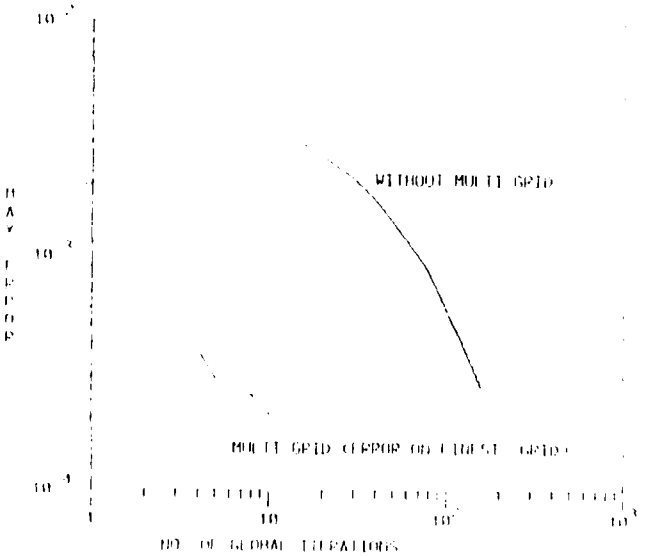

Fig. 2. Convergence Rate with Multi-Grid Scheme (Trough $\alpha = -0.015$, $Re = 8 \times 10^4$).

fine grid initializations. This uni-directional process was still a considerable improvement over direct calculations on the finest grid. Figure 2 depicts the significant reduction in iteration count with the multi-grid procedure. Figure 3 depicts the sensitivity of the pressure solution to mesh width for the trailing edge triple deck interaction. The skin friction is much less grid dependent. This behavior was found for other geometries as well.[4,5] Finally, the convergence rate, for a fixed ξ mesh, as a function of the outer boundary location y_M is shown in figure 4. The results are consistent with the prediction that convergence will deteriorate as $(\Delta\xi/y_M)$ decreases. With the multi-grid correction however (figure 2), this sensitivity is greatly reduced and the parameter $(\Delta\xi/y_M)$ is less critical.

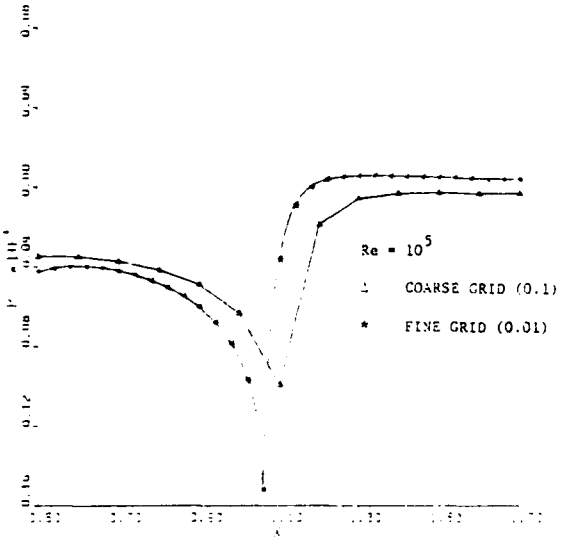

Fig. 3a. Flat Plate Trailing Edge Pressure on Two Grid Levels (Laminar).

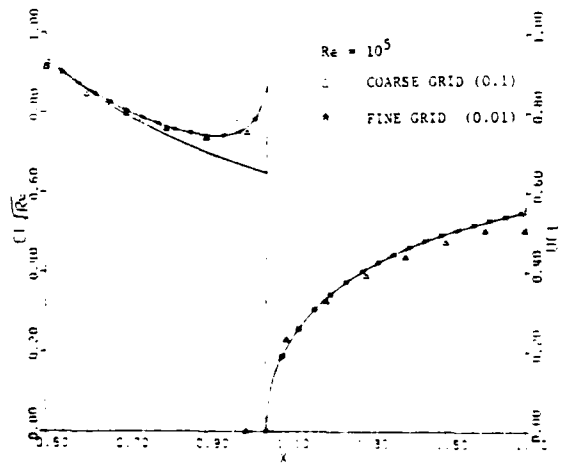

Fig. 3b. Flat Plate Trailing Edge Skin Friction on Two Grid Levels (Laminar).

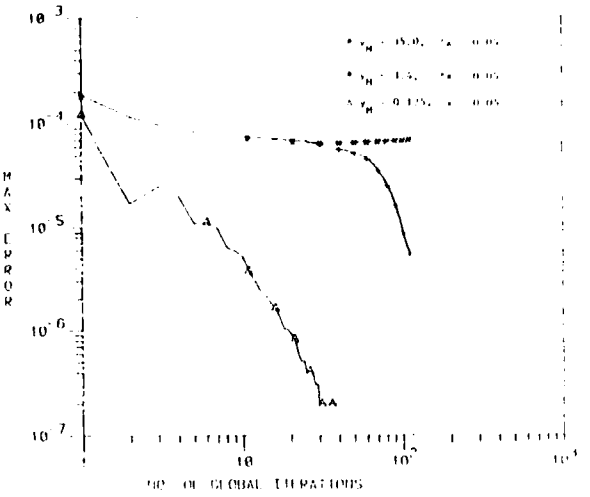

Fig. 4. Convergence Rate for Different $(\Delta x/y_M)$ (Semi-Infinite Flat Plate).

6. Solutions

(i) Inviscid Flow - Boattail

Since the PNS equations are applied here for the evaluation of the complete viscous/inviscid interaction, the effectiveness of the relaxation procedure, for the discrete system (1-5), for inviscid flow is important. For supersonic flow with a fitted shock boundary,[8] the inviscid region is relatively small; however, for subsonic[6] or transonic[7] flows, these regions can be quite extensive and the overall convergence rate of the PNS procedure will be dependent on the "inviscid" convergence properties. In order to test the present method, solutions were obtained for the inviscid flow (slip boundary conditions) over an axisymmetric boattail configuration.[3-5] The results are shown in figure 5, without a multi-grid correction, and compared with potential flow solutions obtained with the CSIP procedure.[15] The initial conditions are somewhat

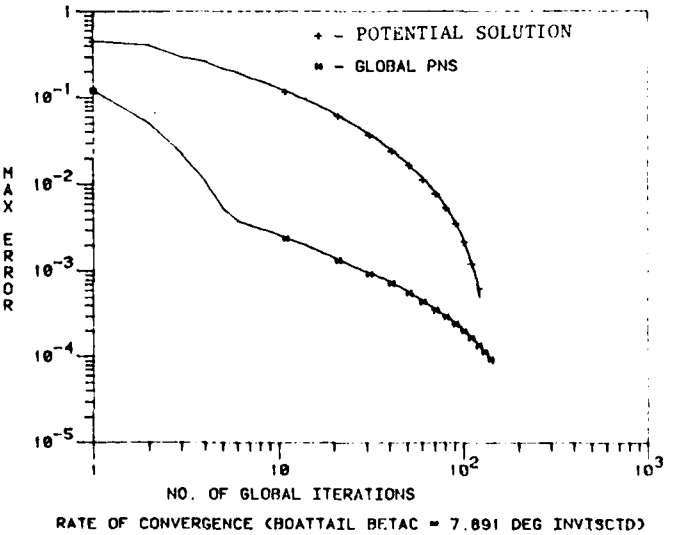

Fig. 5. Convergence Rate for Inviscid Flow On Boattail (Juncture Angle 15.8°).

different and therefore the potential solutions start with a slightly larger error. The figure clearly shows that the convergence rate of the line relaxation procedure for the pressure described herein is not significantly different than that for the potential equation and the CSIP. This is an important and somewhat surprising result. Moreover as seen in figure 6a, the solution is essentially second-order accurate. This was discussed previously; further analysis is given in references 4,5 where it was shown that on the staggered grid of figure 1, the inviscid discrete equations for the pressure and velocities are in error by $O(\Delta\xi^2, \Delta\eta^2)$, when the vorticity is defined by

$$\omega_{i,j} = \frac{v_{i+1,j} - v_{i,j} + v_{i+1,j-1} - v_{i,j-1}}{2\Delta\xi} - \frac{u_{i,j} - u_{i,j-1}}{\Delta\eta} .$$

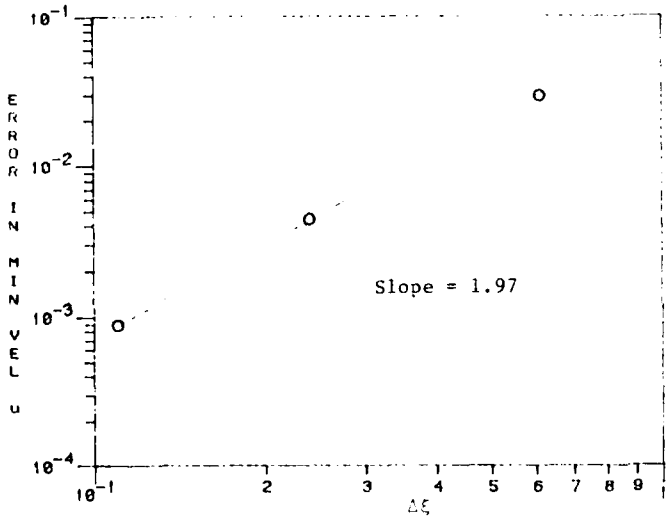

Fig. 6a. Accuracy Plot for Inviscid Flow on Boattail (Juncture Angle 15.8°).

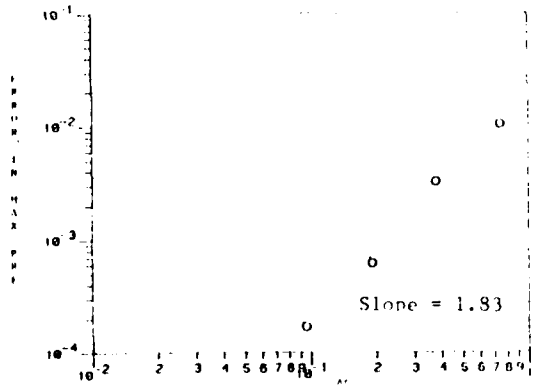

Fig. 6b. Accuracy Plot for Boattail (Juncture Angle 30°) Laminar Flow Re = 1000.

These results confirm the validity and accuracy of the relaxation procedure for inviscid regions. An accuracy plot for the viscous boattail discussed previously[3-5] is given in figure 6b. Note that the exponent 1.8 is obtained. Similar results were found for the trough configuration.[5] This indicates that the overall accuracy of the system (6-8) is, as predicted, somewhere between first and second order.

(ii) Finite Flat Plate - PNS

Solutions for the full PNS system are given in references 3-5 for the laminar incompressible flow over a finite flat plate. The pressure coefficient given in figure 3 for two grids is shown in figure 7. These results are repeated here in order to demonstrate the excellent agreement obtained with interacting boundary layer solutions for this geometry. The trailing edge pressure and skin friction are predicted very accurately and for the staggered grid the minimum pressure is obtained at the trailing edge of the plate. Due to the discontinuity in pressure

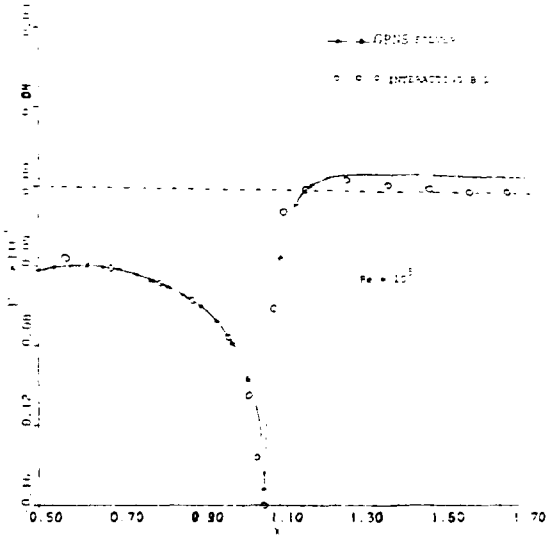

Fig. 7a. Flat Plate Trailing Edge Pressure (Laminar Flow).

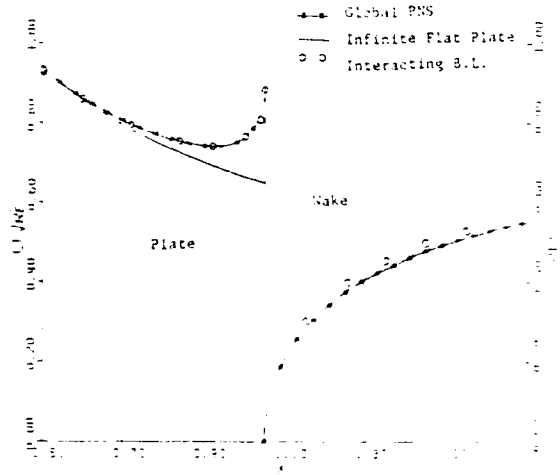

Fig. 7b. Flat Plate Trailing Edge Skin Friction and Wake Centerline Velocity (Laminar).

gradient at the trailing edge, the accuracy factor was 1.35, a value somewhat less than that found for the boattail and trough.

For the present study we are particularly concerned with the trailing edge behavior for turbulent flow conditions. The two-layer Cebeci-Smith eddy viscosity model[16] has been assumed for the Reynolds stress term in the ξ-momentum equations on the plate, and a modified version given in reference 16 has been applied in the wake. Reynolds stresses have been neglected in the η-momentum equation. The two-layer model should be adequate for this unseparated flow problem. Limited interacting boundary layer results have been presented in reference 17. A definitive triple deck theory has not been completed for this flow. One of the open questions concerns the influence of normal pressure gradients.

Solutions for the pressure coefficient, skin friction and wake centerline velocity are shown in figures 8a and 8b. The centerline velocity and pressure results are in reasonable agreement with interacting boundary layer and experimental values.[17,19] The normal pressure gradients at the trailing edge (figures 9a and 9b), however, are quite different than those found for laminar flow, (figure 9a). In the latter case virtually all of the pressure change occurs outside of the boundary layer, i.e., in the inviscid region or outer deck of the triple deck structure. For the turbulent flow, approximately 60% of the pressure change occurs inside the boundary layer (figure 9b). Therefore, the longitudinal pressure distribution (figure 8a) at the surface (centerline) is considerably different than that at the boundary layer edge. This clearly has some implications with regard to the applicability of conventional interacting boundary layer methods that neglect these gradients. Similar effects have been found for the boattail geometry.[4,5] It is surprising that the values of the centerline velocity (figure 8b) are in such good agreement. Further study on the effect of normal pressure gradients for turbulent flow is certainly suggested.

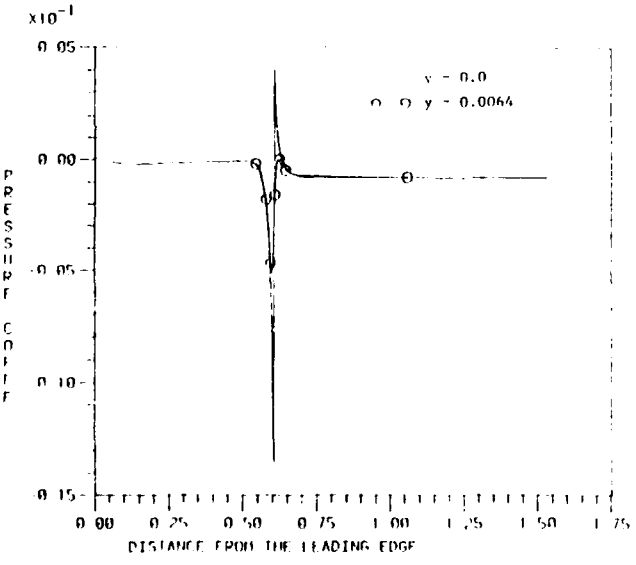

Fig. 8a. Flat Plate Trailing Edge Pressure (Turbulent, Re = 6.5×10^5).

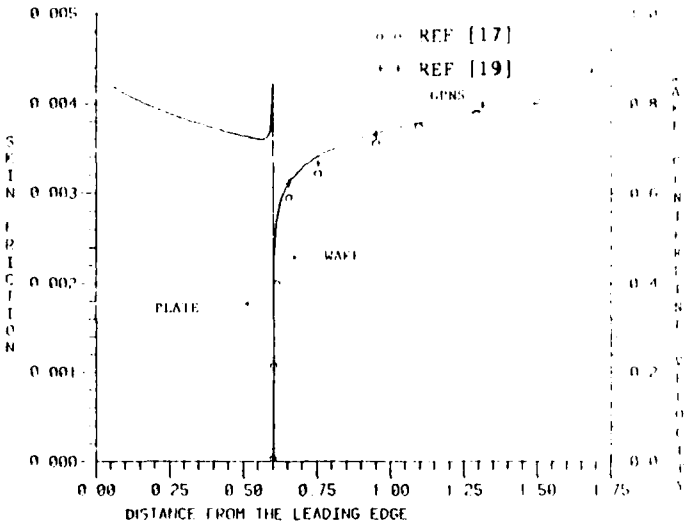

Fig. 8b. Flat Plate Trailing Edge Skin Friction and Wake Centerline Velocity (Turbulent, Re = 6.5×10^5).

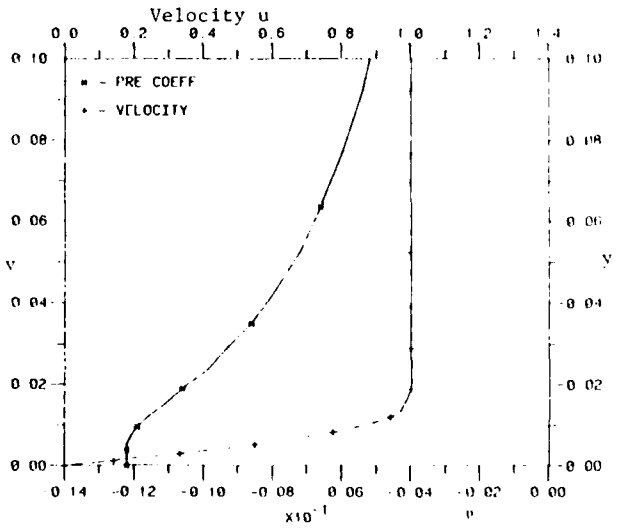

Fig. 9a. Normal Pressure Distribution Near Trailing Edge of Flat Plate (Laminar, Re = 10^5).

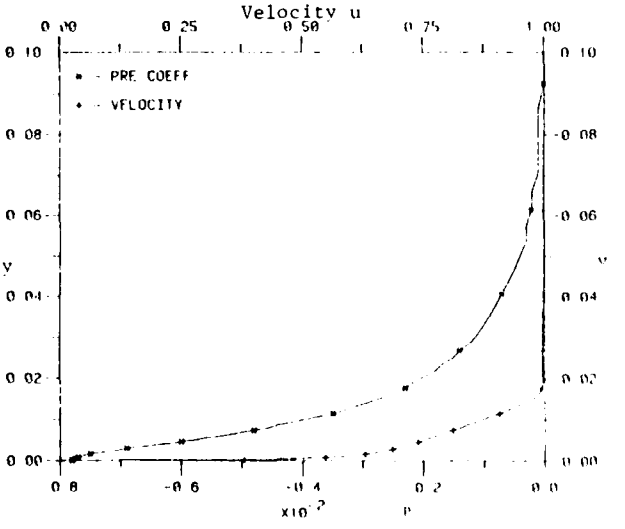

Fig. 9b. Normal Pressure Distribution Near Trailing Edge of Flat Plate (Turbulent, Re = 6.5×10^5).

(iii) NACA 0012 Airfoil - PNS

Laminar and turbulent flow over a NACA 0012 at zero incidence is considered for incompressible and subsonic ($M_\infty = 0.3$) flow. The two-layer eddy viscosity model is applied once again. This should be suitable for non-separated flow; however, for the separated flow solutions, the adequacy of this model could be questioned. For the mild separation regions occurring with the airfoil geometry, the errors incurred with this closure model should be relatively small. This is not true for regions with massive separation zones. The metric h in the governing equations (1-3) is obtained from a conformal mapping procedure described in previous studies.[3-5] The grid is shown in figure 10.

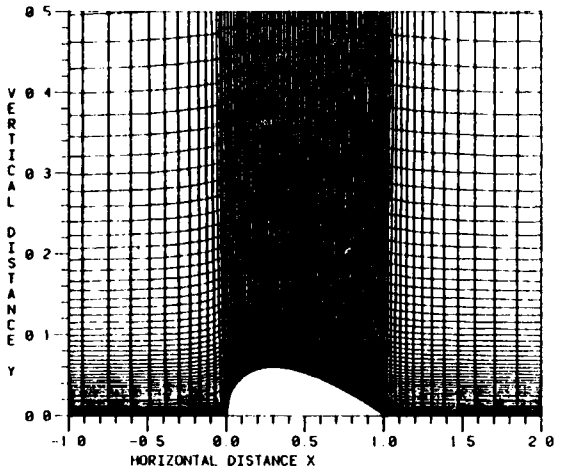

Fig. 10. NACA 0012 Airfoil Grid Close to the Body (Physical Plane).

Laminar flow solutions have been obtained for Reynolds numbers, Re = 5000, 10000, 12500. For the larger value of Re a small separation region appears near the trailing edge, figures 11a, 11b. A detailed study of the front stagnation point for a series of successively finer grids has provided evidence that the PNS approximation, in an appropriate body fitted coordinate system, can accurately evaluate the flow in this region. Recall, that the exact Navier-Stokes equations for stagnation point flow do not include diffusion effects along the surface or diffusion terms in the normal momentum equation. Comparisons of the present PNS stagnation point shear stress with the exact Navier-Stokes value of 1.25 are given for several grids in figure 12. For the finest two grids, the agreement is quite good.

Turbulent flow solutions are shown in figures 13a and 13c for $Re = 5.35 \times 10^5$. Based on experimental data,[18] transition has been prescribed at a distance along the airfoil x/c = 0.4, where c is the chord length. Separation does not occur. The agreement with the data is reasonable (figure 13a) considering the fact that the grid resolution is clearly inadequate for the region x/c = 0.4, where the flow is laminar at the same very large Reynolds number. Finally, the normal pressure gradient for the laminar and turbulent flows is shown in figure 13b,c. Behavior similar to that found for the trailing edge is obtained for the airfoil configuration.

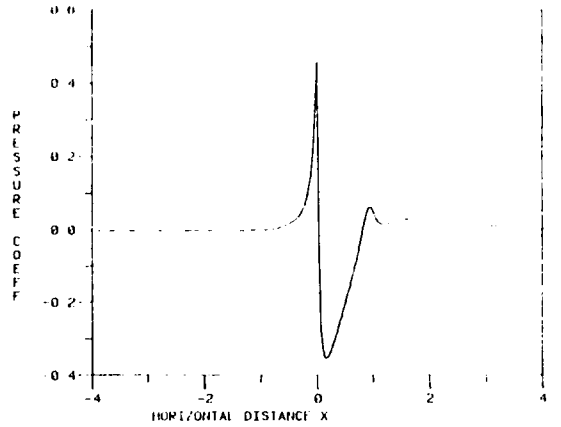

Fig. 11a. NACA 0012 Airfoil, Laminar w (Re = 12,500).

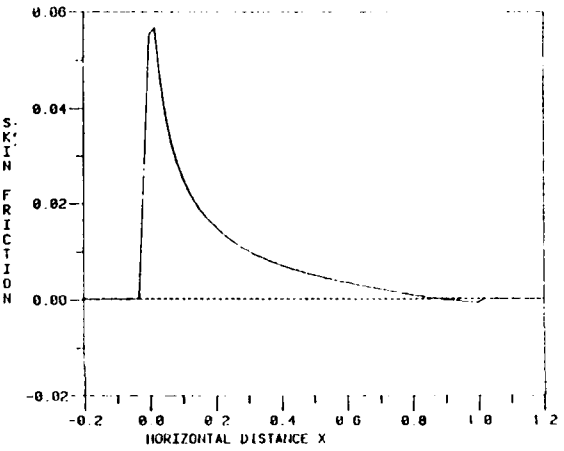

Fig. 11b. NACA 0012 Airfoil, Laminar Flow (Re = 12,500).

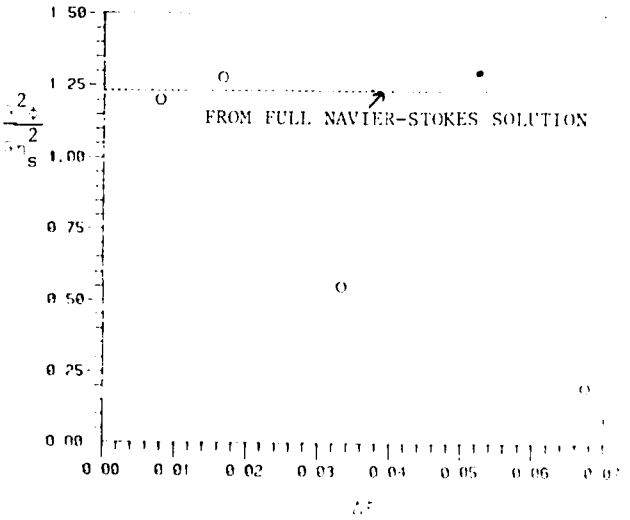

Fig. 12. NACA 0012 Airfoil Stagnation Flow at the Leading Edge (Re = 5000).

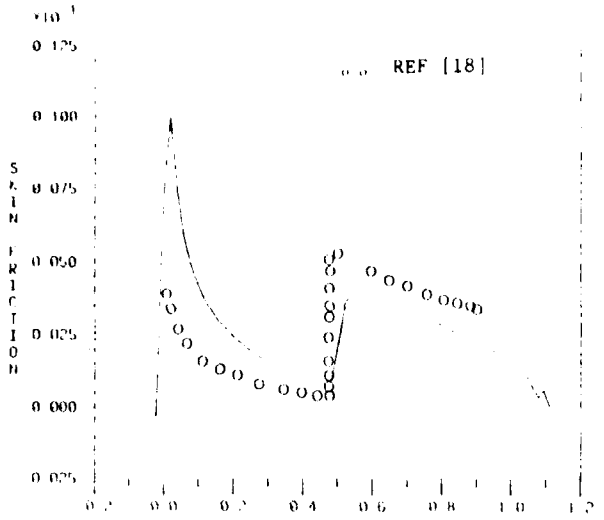

Fig. 13a. NACA 0012 Airfoil Turbulent Flow ($Re = 5.35 \times 10^5$).

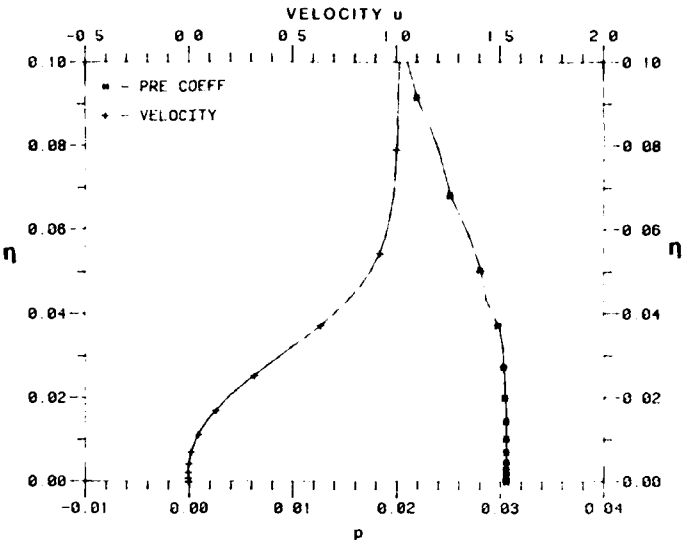

Fig. 13b. Normal Pressure Distribution Near Trailing Edge of NACA 0012 Airfoil (Laminar, $Re = 10^4$).

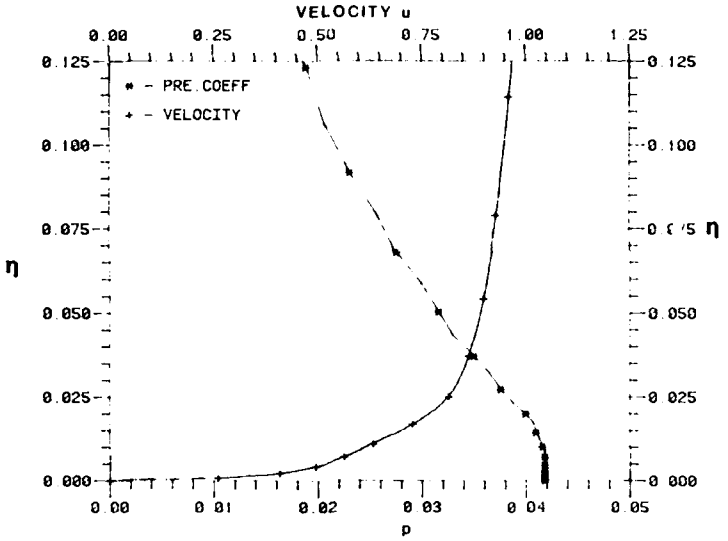

Fig. 13c. Normal Pressure Distribution Near Trailing Edge of NACA 0012 Airfoil (Turbulent, $Re = 5.35 \times 10^5$).

(iv) Other Geometries

Solutions with large separation regions have been presented for the boattail geometry.[5] Both laminar and turbulent flows have been considered. Finally, for subsonic and transonic flow, laminar solutions over a cone-cylinder-boattail configuration, for which separation occurs, have been presented in references 6, 7. Initial results for supersonic flow over a cone have been given in reference 8. Additional supersonic studies will be presented in future papers.

7. Summary

Laminar and turbulent solutions for finite flat plate and NACA 0012 airfoil geometries have been obtained with a multi-sweep PNS relaxation procedure. The method is unconditionally stable, departure free, separation singularity free and describes separation, stagnation point and trailing edge behavior. With the difference equation given on a partially staggered grid, the inviscid equations are second-order accurate and the full PNS system is somewhere between first and second-order. The convergence rate for inviscid flow is comparable to that obtained for the full potential equation. For fine meshes or large values of the upper boundary y_M, the convergence rate slows considerably. A one-dimensional multi-grid procedure for the pressure has been applied in order to alleviate this difficulty. The solutions are in good agreement with previous results or data and the effects of normal pressure gradients for turbulent flows are shown to be significant even within the boundary layer. The method is applicable for flows with strong pressure interaction and large separation

regions when the difference equations are written in an appropriate streamline coordinate system. Other studies for cone, trough, boattail, cone-cylinder-boattail and base flows have established the procedure as applicable for subsonic, transonic and supersonic flow.

Acknowledgement

This research was supported by the Air Force Office of Scientific Research under Grant No. AFOSR-80-0047.

References

1. Rubin, S.G. and Lin, A. (1980), "Marching with the PNS Equations," Proceedings of 22nd Israel Annual Conference on Aviation and Astronautics, Tel Aviv, Israel, pp. 60-61.

2. Rubin, S.G. (1981), "A Review of Marching Procedures for Parabolized Navier-Stokes Equations," Proceedings of a Symposium on Numerical and Physical Aspects of Aerodynamic Flows, Springer-Verlag, 1982, pp. 171-186.

3. Rubin, S.G. and Reddy, D.R. (1983), "Global Solution Procedure for Incompressible Laminar Flow with Strong Pressure Interaction and Separation," presented at the 2nd Symposium on Numerical and Physical Methods for Aerodynamic Flows, Long Beach State University, Long Beach, CA, January 1983, Springer-Verlag.

4. Rubin, S.G. and Reddy, D.R. (1983), "Analysis of Global Pressure Relaxation for Flows with Strong Interaction and Separation," (to appear in Computers and Fluids).

5. Reddy, D.R. (1983), "Global Pressure Relaxation Procedure for Laminar and Turbulent Incompressible Flows with Strong Interaction and Separation," Ph.D. Dissertation, Dept. of Aerospace Engineering and Applied Mechanics, University of Cincinnati.

6. Khosla, P.K. and Lai, H.T. (1983), "Global PNS Solutions for Subsonic Strong Interaction Flows," (to appear in Computers and Fluids).

7. Khosla, P.K. and Lai, H.T. (1983), "Global PNS Solutions for Transonic Strong Interaction Flows," (in preparation).

8. Lin, A. and Rubin, S.G. (1982), "Three-Dimensional Supersonic Viscous Flow Over a Cone at Incidence," AIAA Journal, Vol. 20, No. 11, pp. 1500-1507.

9. Rudman, S. and Rubin, S.G. (1968), "Hypersonic Flow Over Slender Bodies Having Sharp Leading Edges," AIAA Journal, 6, 10, pp. 1883-1890, October 1968.

10. Lin, T.C. and Rubin, S.G. (1973), "Viscous Flow Over a Cone at Moderate Incidence. I," Computers and Fluids, 1, pp. 37-57.

11. Davis, R.T. and Rubin, S.G. (1980), "Non-Navier-Stokes Viscous Flow Computations," Computers and Fluids, 8, 1, pp. 101-132.

12. Lubard, S. and Helliwell, W. (1975), "An Implicit Method for Three Dimensional Viscous Flow with Application to Cones at Angle of Attack," Computers and Fluids, 3, 1, pp. 83-101.

13. Vigneron, Y. et al. (1978), "Calculation of Supersonic Flow Over Delta Wings with Sharp Leading Edges," AIAA Paper No. 78-1137.

14. Brandt, A. (1979), "Multi-Level Adaptive Computations in Fluid Dynamics," AIAA Paper No. 79-1455, Computational Fluid Dynamics Conference, Williamsburg, VA, 1979.

15. Khosla, P.K. and Rubin, S.G. (1982), "A Composite Velocity Procedure for the Compressible Navier-Stokes Equations," AIAA Paper No. 82-0099.

16. Cebeci, T. et al. (1979), "On the Calculation of Symmetric Wakes. I. Two-Dimensional Flows," Numerical Heat Transfer, Vol. 2, pp. 35-60.

17. Vatsa, V.N., Werle, M.J. and Verdon, J.M. (1981), "Analysis of Laminar and Turbulent Symmetric Blunt Trailing-Edge Flows," United Technologies Research Center, East Hartford, CT, Report No. R81-914986-5.

18. von Doenhoff, A.E. (1940), "Investigation of the Boundary Layer About a Symmetric Airfoil in a Wind Tunnel of Low Turbulence," NACA Wartime Report L-507.

19. Chevray, R. and Kovasznay, L.S.G. (1969), "Turbulent Measurements in the Wake of a Thin Flat Plate," AIAA Journal, Vol. 7, No. 8, pp. 1641-1643.

END

FILMED

3-84

DTIC